

Light-quark baryons

Volker Burkert¹, Eberhard Klempt² and Ulrike Thoma²

¹Thomas Jefferson National Accelerator Facility, 12000 Jefferson Avenue, Newport News, Virginia 23606, USA

²Helmholtz-Institut für Strahlen- und Kernphysik, Universität Bonn, Germany

Received: December 27, 2022/ Revised version:

Abstract. This is a contribution to the review “50 Years of Quantum Chromodynamics” edited by F. Gross and E. Klempt, to be published in EPJC. The contribution reviews the new baryon resonances derived from photoproduction experiments. Implications of the new results for the interpretation of baryons are discussed.

1 Why N^* ’s?

This was the question with which Nathan Isgur opened his talk at N^*2000 [1] held at the Thomas Jefferson National Accelerator Facility in Newport News, VA, one year before he passed away, much too early. He gave three answers:

First, nucleons are the stuff of which our world is made. The N^* ’s and Δ^* ’s are of great importance in the development of the Universe, when hadrons materialized from a soup of quarks and gluons at some $10\,\mu\text{s}$ after the big bang. The full spectrum of excited baryon states including those carrying strangeness must be included in hadron gas models that simulate the freeze-out behavior observed in hot-QCD calculations. These simulations aim at finding the underlying processes, to pin-point the “critical point” of the phase transition that is expected to occur between the QGP phase and the hadron phase at a temperature near 155 MeV. Experiments are ongoing at CERN, RHIC and planned at FAIR to study the phase diagram of strongly interacting matter, e.g. by varying the collision energy.

Second, nucleons are the simplest system in which the non-abelian character of QCD is manifest. The proton consists of three (constituent) quarks since the number of colors is three.

Third, baryons are sufficiently complex to reveal physics to us hidden in the mesons. Gell-Mann and Zweig did not develop their quark model along mesons, their simple structure allowed for different interpretations. *Three* quarks resulted in a baryon structure that gave - within SU(3) symmetry - the octet and the decuplet containing the famous Ω^- .

Isgur made many important contributions to the development of the quark model. With Karl he developed the idea that gluon-mediated interactions between quarks bind them into hadrons and constructed a quark model of baryons [2]. This was a non-relativistic model, hardly justifiable. With Capstick he relativized the model [3], but

surprisingly, the pattern of predicted resonances remained rather similar. Isgur always defended the basic principles: hadrons have to be understood in terms of constituent quarks bound in a confining potential and additionally interacting via the exchange of “effective” gluons.

Nearly 20 years later, Meißner ended his contribution [4] to the N^*2019 conference held in Bonn, Germany, by stating: “Forget the quark model”. We need to ask: What has happened in these two decades? What did we know before? What have we learned?

Mapping the excitation spectrum of the nucleon (protons and neutrons) and understanding the effective degrees of freedom are important and most challenging tasks of hadron physics. A quantitative description of the spectrum and properties of excited nucleons must eventually involve solving QCD for a complex strongly interacting multi-particle system. The experimental N^* program currently focuses on the search for new excited states in the mass range just below and above 2 GeV using energy-tagged photon beams in the few GeV range, and on the study of resonances, their properties, and their internal structure, e.g. in cascade decays and in meson electroproduction.

2 N^* ’s: how?

The expected spectrum of nucleon and Δ excitations is rather rich. Even in the lowest excitation mode with $l_\rho = 1$ or $l_\lambda = 1$, we expect five N^* and two Δ^* states; they are all well established. But already in the second excitation mode, the quark model predicts 13 N^* and 8 Δ^* states. The resonances have quantum numbers $J^P = 1/2^+, \dots, 7/2^+$ and isospin $I = 1/2$ or $3/2$, respectively. All these 21 resonances are expected to fall into a mass range of, let’s say, 1600 - 2100 MeV. This complexity of the light-quark (u & d quarks) baryon excitation spectrum complicates the experimental search for individual

states, especially since, as a result of the strong interaction, these states are broad, the typical width being 150-300 MeV. They overlap, interfere, and often several resonances show up in the same partial wave. Compared to $\pi\pi$ scattering experiments, additional complications due to the nucleon spin emerge in πN elastic scattering. Now there are two complex amplitudes to be determined, for spin-flip and spin-non-flip scattering.

Pion scattering off nucleons was mostly performed in the pre-QCD era. Nearly all excited nucleon states listed in the Review of Particle Physics (RPP) prior to 2012 have been observed in elastic pion scattering $\pi N \rightarrow \pi N$. However there are important limitations in the sensitivity to the higher-mass nucleon states. These may have very small $\Gamma_{\pi N}$ decay widths, and their identification becomes exceedingly difficult in elastic scattering. Three groups extracted the real and imaginary parts of the πN partial-wave amplitude from the data [5–7]. Their results are still used as constraints in all modern analyses of photo-induced reactions.

Figure 1a,b shows the real and imaginary part of the S_{11} amplitude for πN scattering. The imaginary part peaks at 1500 MeV and just below 1700 MeV indicating the presence of two resonances, $N(1535)1/2^-$ and $N(1650)1/2^-$. These are known since long and established. Above, there is no clearly visible sign for any additional resonance. Higher-mass resonances – if they exist – must have very small $\Gamma_{\pi N}$ decay widths.

Estimates for alternative decay channels have been made in quark model calculations [13]. This has led to major experimental efforts at Jefferson Lab, ELSA and MAMI to determine differential cross sections and (double) polarization observables for a variety of meson photoproduction channels. Spring-8 at Sayo in Japan and the ESRF in Grenoble, France, made further contributions to the field.

Figure 1c,d shows an example. In Fig. 1c, the total cross section for η photoproduction off protons and off neutrons is shown [8,9]. They are dominated by $N(1535)1/2^- \rightarrow N\eta$ interfering with $N(1650)1/2^-$. The opening of important channels is indicated by vertical lines. At the η' threshold, the intensity suddenly drops: significant intensity goes into the $N\eta'$ channel. This is a strong argument in favor of a resonance at or close to the $p\eta'$ threshold. It also clearly demonstrates the advantage of investigating different final states and production mechanisms. In contrast to the πN - S_{11} scattering amplitude, here, already in the total η -photoproduction cross section, a structure relating to $N(1895)1/2^-$ becomes visible. Furthermore, in Fig. 1d, the result of a fit with Legendre moments to the so-called Σ polarization observable for $\gamma p \rightarrow \eta p$ is compared to two energy-dependent solutions of the BnGa coupled-channel analysis. Plotted is the coefficient $(a_4)_4^\Sigma$ of the Legendre expansion which receives (among others) a contribution from the interference of the S -wave with the G -wave. Data from different experiments are given with their error bars. The curves represent BnGa fits with (solid curve) and without (dashed curve) inclusion of data on $\gamma p \rightarrow \eta' p$. The $N(2190)7/2^-$ (G -wave) was included in

both fits. From 1750 MeV to the $p\eta'$ -threshold the coefficient is approximately constant, then at the $p\eta'$ -threshold, the fit result shows an almost linear rise towards positive values. This change of the coefficient at about 1.9 GeV indicates the presence of a cusp. The strong cusp is an effect of the $p\eta'$ threshold [$E_\gamma = 1447$ MeV ($W = 1896$ MeV)], the $N\eta'$ amplitude must be strongly rising above threshold. Indeed, the inclusion of the full data set on $\gamma p \rightarrow p\eta'$ (cross sections, polarization observables) into the BnGa data base had already confirmed the existence of a new $N(1895)1/2^-$ resonance with a significant coupling to $p\eta$ and $p\eta'$ [14, 15], first observed in [16].

This resonance was not seen in classical analyses of πN elastic scattering data¹. The example shows the importance of inelastic channels and of coupled-channel analyses. Thresholds can be identified by the missing intensity in other channels, cusp effects can show up, all these effects need to be considered and finally contribute to find the correct solution. High-precision and high-statistics data are required as well as a large body of different polarization data.

3 Photoproduction of exclusive final states

In the photoproduction of a single pseudoscalar meson like $\gamma p \rightarrow \eta p$, not only the proton has two spin states but also the photon has two possible spin orientations. In electroproduction, the virtual photon can also be polarized longitudinally. But even for experiments with real photons, there are four complex amplitudes to be determined. There is a large number of observables: the target nucleon can be polarized longitudinally, i.e. in beam direction, or transversely, the photon can carry linear or circular polarization. The final-state nucleon can carry polarization along its flight direction or perpendicular to the scattering plane. There is an intense discussion in the literature on how many independent measurements have to be performed to determine the four complex amplitudes, see Ref. [20]. In practice, energy-independent analyses in bins of the invariant mass were only done for the very low energy region [21, 22] or with additional assumptions (see [23–25] and references therein).

In most cases, energy-dependent analyses have been performed to extract the information hidden in the photoproduction data. Here the polarization data, in particular those with polarized photon beam and polarized target nucleons, were decisive to reduce ambiguities of the solutions. The double polarisation observable E is one of the beam-target-observables; it requires a circularly polarized photon beam and a longitudinally polarized target. Examples of E for selected W -bins are shown in Fig. 2 for $\gamma p \rightarrow p\eta$ [11]. The data are compared to the predictions of different PWA solutions (colored curves). The curves scatter over a wide range indicating the high sensitivity of the polarisation observable on differences in the contributing amplitudes. A new BnGa fit returned masses

¹ Höhler and Manley had claimed a similar state that had been combined with Cutkovsky's result to $N(2090)$.

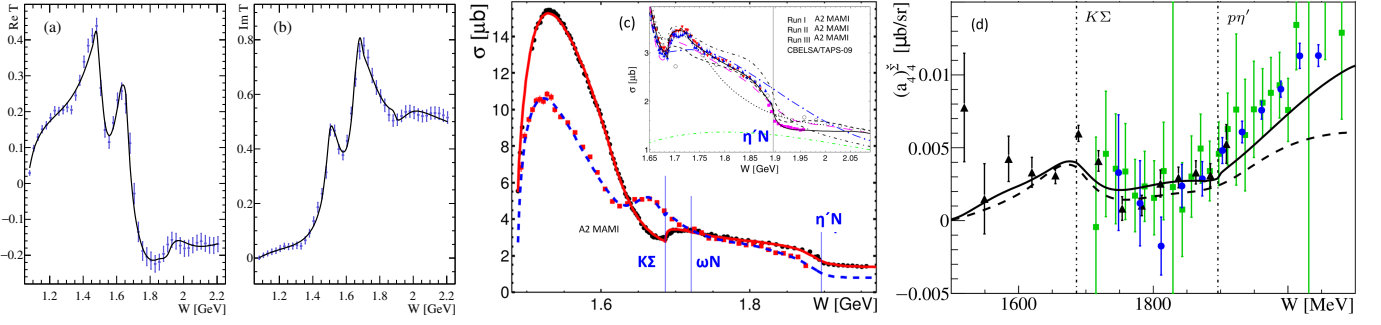


Fig. 1. (a),(b): Real and imaginary part of the S_{11} πN scattering amplitude. Resonances in this partial wave have quantum numbers $J^P = 1/2^-$. Clearly seen are $N(1535)1/2^-$ and $N(1650)1/2^-$. There is no convincing evidence for any resonance above 1700 MeV. Data points are from [5], errors are estimates, the curve represents a recent Bonn-Gatchina (BnGa) fit. (c): Total cross sections for $\gamma p \rightarrow \eta p$ and $\gamma n \rightarrow \eta n$. Important thresholds are marked by lines. The inset shows the η' threshold region for η' -photoproduction off the proton (picture adapted from [8,9]). (d): The Legendre coefficient of the polarization observable Σ (a_4^{Σ}) exhibits a cusp at the η' threshold [10]. The data stems from GRAAL (black), CBELSA/TAPS (blue) and CLAS (green). Picture taken from [10]. (c),(d): see publications [8,9,11] for references to the data.

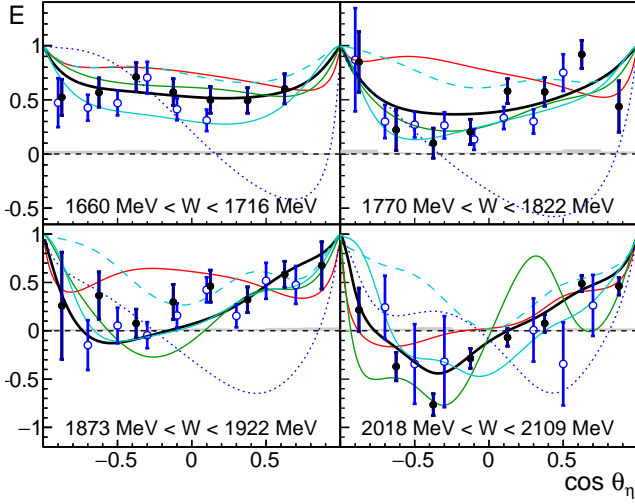


Fig. 2. The double polarization observable E as a function of $\cos \theta_n$ in the cms for selected energy bins, black: CBELSA/TAPS [11], blue: CLAS data [12] (due to different binning, the energies differ by up to half of the bin size). Colored curves: Predictions from different PWAs (see publication for references), black: BnGa-fit including the data shown here and further new polarization data. Figure adapted from [11].

and widths of N^* -resonances and their $N\eta$ -branching fractions [11], several of them unknown before. Interestingly a $N(1650)1/2^- \rightarrow N\eta$ -branching fraction of 0.33 ± 0.04 was found while in the RPP'2010, a value of only 0.023 ± 0.022 was given. Recently, also within the Jülich-Bonn dynamical coupled channel approach, a $N\eta$ -residue for $N(1650)1/2^-$ was found, larger by almost a factor of two compared to earlier analyses, after inclusion of the new polarisation data [26]. Historically, the large $N(1535)1/2^- \rightarrow N\eta$ branching fraction and the small one for $N(1650)1/2^- \rightarrow N\eta$ has played a significant role in the development of the quark model [27], of theories based on coupled-channel chiral effective dynamics [28] and led to several interesting interpretations of the low mass $1/2^-$ -resonances (for ref-

erences see [11]). The old values from 2010 were obtained without the constraints provided by the new high quality (double) polarization data covering almost the complete solid angle. The impact of polarization observables on the convergence of different PWA-solutions was e.g. also very clearly demonstrated in a common study of pion-photoproduction [29].

In hyperon decays, the polarization of the Λ or Σ^0 can be determined by analyzing the parity violating decay $\Lambda \rightarrow p\pi^-$. Thus the spin orientation of the final state baryon (the recoil polarization) can be determined. Kaon-hyperon production using a spin-polarized photon beam provides access to the beam-, recoil-, target-² and to beam-recoil polarization observables. The data had a significant impact on the determination of the resonance amplitudes in the mass range above 1.7 GeV. Precision cross section and polarization data, examples of which are shown in Figure 3, span the $K^+\Lambda$ and $K^+\Sigma$ invariant mass range from threshold to 2.9 GeV, hence covering the interesting domain where new states could be discovered. Clear resonance-like structures at 1.7 GeV and 1.9 GeV are seen in the $K^+\Lambda$ -differential cross section that are particularly prominent and well-separated from other structures at backward angles. At more forward angles (not shown) t-channel processes become prominent and dominate the cross section. The broad enhancement at 2.2 GeV may also indicate resonant behavior although it is less visible at more central angles with larger background contributions. Similar resonance-like structures are observed in the $K\Sigma$ channel (Figure 3(b)). Examples for different polarisation observables determined for the reaction $\gamma p \rightarrow K^+\Lambda$ are shown in the lower row of Figure 3 for selected bins in the K^+ -scattering angle in the γp center-of-mass frame. They are compared to predictions from ANL-Osaka, BnGa-2014 and to a refit from the BnGa-PWA. The large differences

² The target polarisation observable can also be accessed by performing a double polarization experiment using a linearly polarised photon beam and measuring the baryon polarisation in the final state.

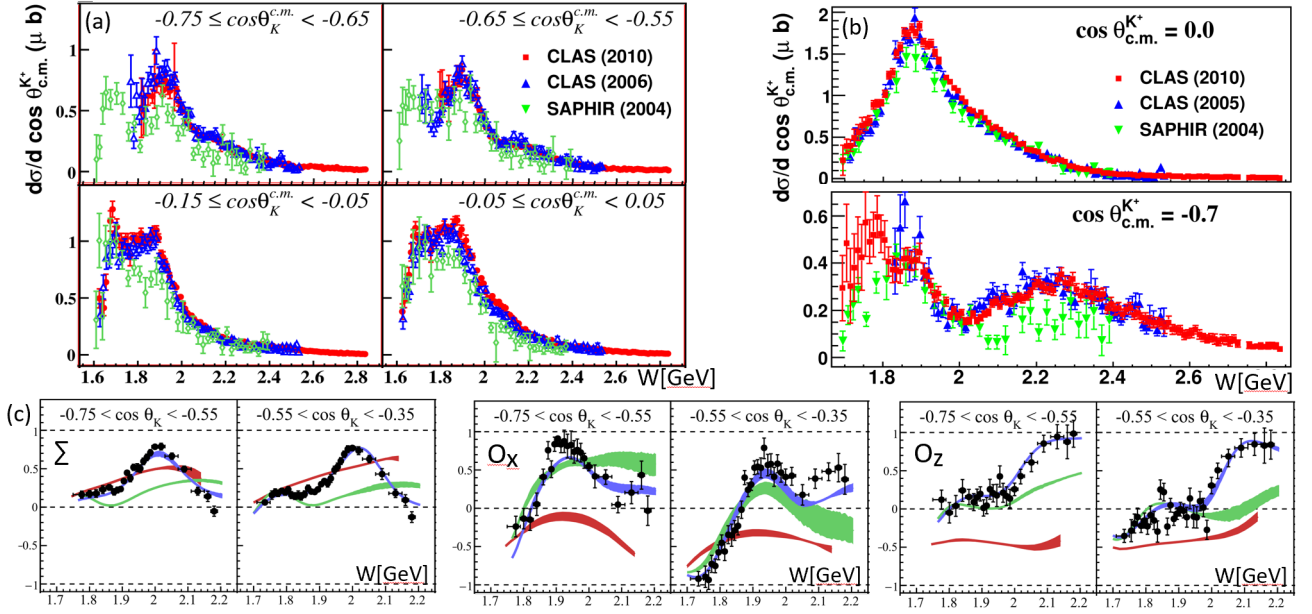


Fig. 3. Invariant mass dependence of the $\gamma p \rightarrow K^+ \Lambda$ [17] (a) and $\gamma p \rightarrow K^+ \Sigma$ [18] (b) differential cross sections for selected bins in the polar angle. (c) Examples for polarization observables determined for $\gamma p \rightarrow K^+ \Lambda$ (only selected bins shown) [19]. Curves: PWA-predictions from ANL-Osaka (red) and BnGa 2014 (green). Blue: BnGa 2014-refit including the data shown. (a)-(c): For references to the data and the PWAs see [17–19], Picture adapted from [17–19]

between the curves demonstrate the sensitivity of the data to the underlying dynamics. The $K\Lambda$ channel is somewhat easier to understand than the $K\Sigma$ channel, as the iso-scalar nature of the Λ selects isospin-1/2 states to contribute to the $K\Lambda$ final state, while both isospin-1/2 and isospin-3/2 states can contribute to the $K\Sigma$ final state. Of course, here, as well as for other final states, only a full partial wave analysis can determine the underlying resonances, their masses and spin-parity. Polarization data are required to disentangle the different amplitudes.

Energy-dependent analyses have been performed e.g. at GWU [30] as SAID, in Mainz as MAID [9], at Kent [31], at JLab [32], by the BnGa [16,33], the Jülich-Bonn (JüBo) [26], the ANL-Osaka [34] and by other groups. A short description of the different methods can be found in Ref. [20]. Here we emphasize that the energy-dependence of a partial-wave amplitude for one particular channel is influenced by other reaction channels due to unitarity constraints. To fully describe the energy-dependence of a production amplitude, all (or at least the most significant) reaction channels must be included in a coupled-channel approach. Many different final states have been measured with high precision off protons and partly also off neutrons (bound in a deuteron with a quasi-free proton in the final state). Polarization data for meson photoproduction off neutrons are, however, still scarce. A fairly complete list of references can be found in [20]. Most data are now included in single- and in multi-channel analyses³.

³ A list of data on photoproduction reactions including polarization and double-polarization observables can be found at the BnGa web page: <https://pwa.hiskp.uni-bonn.de/>

The photoproduction data had a strong impact on the discovery of several new baryon states or provided new evidence for candidate states that had been observed previously but lacked confirmation (e.g. [9, 16, 35]). Many new decay modes were discovered, in particular in the photoproduction of $2\pi^0$ and $\pi^0\eta$ ([33, 36, 37] and references therein). At the NSTAR’2000 workshop, 12 N^* and 8 Δ^* were considered to be established ($4^*, 3^*$) by

Table 1. Baryon resonances above the $\Delta(1232)$ and below 2300 MeV given in the RPP’2022 in comparison to the resonances considered in the RPP’2010. Resonances with 4^* in 2010 are not listed here. See text for further discussion.

	RPP 2010	RPP 2022		RPP 2010	RPP 2022
$N(1700)3/2^-$	***	***	$\Delta(1600)3/2^+$	***	****
$N(1710)1/2^+$	***	****	$\Delta(1750)1/2^+$	*	*
$N(1860)5/2^+$	—	**	$\Delta(1900)1/2^-$	**	***
$N(1875)3/2^-$	—	***	$\Delta(1920)3/2^+$	***	***
$N(1880)1/2^+$	—	***	$\Delta(1930)5/2^-$	***	***
$N(1895)1/2^-$	—	****	$\Delta(1940)3/2^-$	*	**
$N(1900)3/2^+$	**	****	$\Delta(2000)5/2^+$	**	**
$N(1990)7/2^+$	**	**	$\Delta(2150)1/2^-$	*	*
$N(2000)5/2^+$	**	**	$\Delta(2200)7/2^-$	*	***
$N(2040)3/2^+$	—	*			
$N(2060)5/2^-$	—	***	$N(2080)3/2^-$	**	—
$N(2100)1/2^+$	*	***	$N(2090)1/2^-$	*	—
$N(2120)3/2^-$	—	***	$N(2200)5/2^-$	**	—

the Particle Data Group⁴. These numbers increased to 19 N^* and 10 Δ^* two decades later. Table 1 lists the new resonances below 2300 MeV and those that had not a four-star status in 2010. Resonances which had four stars in 2010 are well established and kept their status. These are: $N(1440)1/2^+$, $N(1520)3/2^-$, $N(1535)1/2^-$, $N(1650)1/2^-$, $N(1675)5/2^-$, $N(1680)5/2^+$, $N(1720)3/2^+$, $N(2190)7/2^-$, $N(2220)9/2^+$, $N(2250)9/2^-$, $\Delta(1620)1/2^-$, $\Delta(1700)3/2^-$, $\Delta(1905)5/2^+$, $\Delta(1910)1/2^+$, $\Delta(1950)7/2^+$. A few resonances were removed from the RPP tables. They often had wide-spread mass values, and the old results were redistributed according to their masses and the new findings. Even more impressive is the number of reported decay modes. Our knowledge on N^* and Δ^* decays has at least been doubled.

4 Regge trajectories

Like mesons, baryons fall onto linear Regge trajectories when their squared masses are plotted as a function of their total spin J or their intrinsic orbital angular momentum L . In the case of Δ^* , the leading trajectory consists of $\Delta(1232)3/2^+$, $\Delta(1950)7/2^+$, $\Delta(2420)11/2^+$, $\Delta(2950)15/2^+$. In the quark model, these have intrinsic orbital angular momenta $L = 0, 2, 4, 6$. Figure 4 shows the squared Δ^* -masses as a function of $L + N_{\text{radial}}$, where N_{radial} indicates the intrinsic radial excitation. The resonances $\Delta(1910)1/2^+$, $\Delta(1920)3/2^+$, $\Delta(1905)5/2^+$ have intrinsic $L = 2$ like $\Delta(1950)7/2^+$, and fit onto the trajectory. Also, there are three positive-parity resonances that likely have $L = 4$ with the $5/2^+$ state missing. The two $L = 1$ resonances $\Delta(1620)1/2^-$ and $\Delta(1700)3/2^-$ also have masses close to the linear trajectory. Further, there are resonances in which the ρ or λ oscillator is excited radially to $n_\rho = 1$ or $n_\lambda = 1$ ($N_{\text{radial}} = 1$). Quark models with a harmonic oscillator as confining potential predict that resonances belong to shells. Radial excitations are predicted in the shell $L+2N_{\text{radial}}$. This is not what we find experimentally: the masses are approximately proportional to $L + N_{\text{radial}}$ if $N_{\text{radial}} = 1$ is assigned to $\Delta(1600)3/2^+$, the first radial excitation of $\Delta(1232)3/2^+$, as well as to the $\Delta(1900)1/2^-$, $\Delta(1940)3/2^-$, $\Delta(1930)5/2^-$ triplet, to the two members of a partly unseen quartet $\Delta(2350)5/2^-$ and $\Delta(2400)9/2^-$, and to $\Delta(2750)13/2^-$ (with $L=5$, $S=3/2$ and $N_{\text{radial}}=1$).

Clearly, this is a very simplified picture of the Δ^* spectrum. The picture is that of the non-relativistic quark model – nobody understands why it works⁵. Resonances – assumed to have the same mass if spin orbit-coupling is neglected – have indeed somewhat different masses. But the gross features of the spectrum of Δ^* resonances are well reproduced.

The nucleon spectrum is more complicated. First, there are more resonances, and second, there are two-quark con-

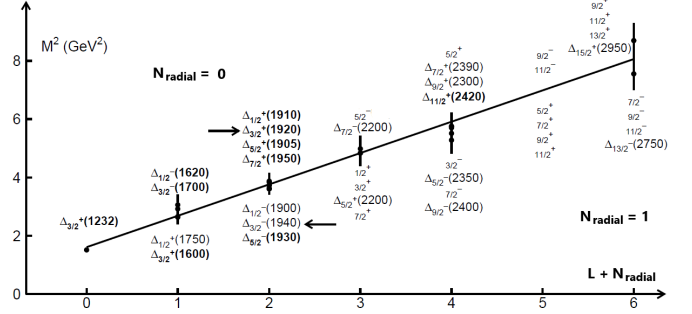


Fig. 4. Regge-like trajectory of Δ^* -resonances. Taken from [42]

figurations which are antisymmetric in spin and flavor⁶. Due to instanton induced interactions, the relativistic quark model [38], expects a lowering of states with the respective symmetry. Indeed baryons with two-quark configurations which are antisymmetric in spin and flavor (*good diquarks*) seem to have lower masses than those having *bad diquarks* only. Attempts to include *good-diquark* effects were rather successful [39, 40]. The χ^2 for the model-data comparison was twice better for the 2-parameter fit than for quark models [41] when the same mass-uncertainties are assumed.

5 Hyperons

Nearly no new data on $\bar{K}N$ scattering have become available for several decades except some new data from BNL at very low energy (see Ref. [43] and references therein). The reaction $\gamma p \rightarrow K^+ \Sigma \pi$ was studied at JLab and helped to understand the low-energy region [44]. However, four groups have re-analyzed K^-p reactions using extensive collections of the old data. The new analysis progress was pioneered by the Kent group which performed a comprehensive partial wave analysis [45, 46]. Energy-independent amplitudes were constructed by starting from an energy-dependent fit and by freezing or releasing sets of amplitudes. The resulting amplitudes were then fit in a coupled-channel approach. The JPAC group performed coupled-channel fits to the partial waves of the Kent group. The fit described the Kent partial waves well while significant discrepancies showed up between data and the observables calculated from their partial-wave amplitudes [47]. The ANL-Osaka group used the data set collected by the Kent group and derived energy-dependent amplitudes based on a phenomenological SU(3) Lagrangian. Two models were presented which agreed for the leading contributions but which showed strong deviations for weaker contributions [48, 49]. The BnGa group added further data and tested systematically the inclusion of additional states with any set of quantum numbers. Only small improvements in the fit were found [50, 51].

⁴ In PDG notation: 4* Existence certain, 3* almost certain, 2* evidence fair, 1* poor

⁵ In addition, we neglect the possible configuration mixing of states in our discussion.

⁶ These two-quark configurations are often called *good diquarks*. They may carry orbital-angular momenta, these are not *frozen* diquarks.

The new studies of old data did not change the situation significantly. Some new decay modes were reported, some new but faint signals were found, some were confirmed by one group and missed by others. Several *bumps* were removed from the RPP Tables (for details see [52]). As a result, our picture of hyperons (with strangeness $S = -1$) remains unclear. Not even all states expected in the first Λ and Σ excitation shell have been seen. In Table 2 all candidates are included.

Very little is known about excited Cascade baryons. A few structures in invariant mass spectra were observed, nearly no spin-parities have been determined. The hope is that at FAIR, JLab and J-PARC new Ξ 's and Ω 's will be observed and their quantum numbers be determined.

6 QCD expectations

The spectrum of excited nucleons has been calculated in different approaches. We list a few here: QCD on a lattice has been used to calculate the spectrum of light-quark baryons including hybrid states [53]. In the Dyson-Schwinger/Bethe-Salpeter approach [54] the covariant three-body Fadeev-equation is solved in a rainbow-ladder approximation. The spectra of baryon resonances have been calculated for $J = 1/2^\pm$ and $J = 3/2^\pm$, reaching for the N^* - and Δ^* -resonances to masses up to about 2000 MeV. AdS/QCD [55] predicts a spectrum of N^* and Δ^* that is proportional to $L + N_{\text{radial}}$. Using chiral unitary approaches for the meson-baryon interactions, certain baryon resonances can be generated dynamically. Various quark models have been developed that treat baryons as bound states of three quarks with constituent masses, a confinement potential and residual quark-quark interactions. At present, they are still best suited to discuss what has been learned from recent results in the spectroscopy of light baryons.

7 What did we learn within the quark model?

7.1 $\text{SU}(6) \otimes \text{O}(3)$ classification

Table 2 lists the observed N^* -, Δ^* -, Λ^* - and Σ^* -baryons in a $\text{SU}(6) \otimes \text{O}(3)$ classification. This classification assumes non-relativistic constituent quarks. It has been a miracle since the early times of the quark model that this scheme works so well. But baryon resonances often have a leading component in the wave function corresponding to the $\text{SU}(6) \otimes \text{O}(3)$ classification even in relativistic calculations. The first excitation shell ($N=1$) is fairly complete. As expected, there are five N^* 's and two Δ^* 's with negative parity. Of the Λ and Σ octet states with negative parity, only the $J^P = 3/2^-$ states are missing⁷. The two states $\Lambda(1800)1/2^-$ and $\Sigma(1750)1/2^-$ are interpreted as states with intrinsic spin $3/2$: they seem to be spin partners of

Table 2. The spectrum of N , Δ , Λ and Σ excitations. The first row shows the quantum numbers of the $\text{SU}(6) \otimes \text{O}(3)$ symmetry group. D is the dimensionality of the $\text{SU}(6)$ group, L the total internal quark orbital angular momentum, P the parity, N a shell index, S the total quark spin, J the total angular momentum. The assignment of particles to $\text{SU}(6) \otimes \text{O}(3)$ is an educated guess. In the first and second excitation band, all expected states are listed, missing resonances are indicated by a $-$ sign. The third band lists only bands for which at least one candidate exists. The states with an index are special: above 1700 MeV, one pair of Σ states is expected at about 1750 to 1800 MeV, two pairs at about 2000 to 2050 MeV. Two pairs marked^a are found only. The pairs are shown with the three possible assignments. Likewise, $N(2060)$ and $N(2190)$ marked^b could form a spin-doublet or be members of a spin-quartet. Likely, the observed pairs of states are mixtures of these allowed configurations (Adapted from [52]).

$(D, L_N^S) J^P$	Singlet	Octet			Decuplet	
$(56, 0_0^+) \frac{1}{2}^+$		$N(939)$	$\Lambda(1116)$	$\Sigma(1193)$	$\Delta(1232)$	$\Sigma(1385)$
$(70, 1_1^-) \frac{1}{2}^-$	$\Lambda(1405)$	$N(1535)$	$\Lambda(1670)$	$\Sigma(1620)$	$\Delta(1620)$	$\Sigma(1900)^a$
$(70, 1_1^-) \frac{3}{2}^-$	$\Lambda(1520)$	$N(1520)$	$\Lambda(1690)$	$\Sigma(1670)$	$\Delta(1700)$	$\Sigma(1910)^a$
$(70, 1_1^-) \frac{5}{2}^-$		$N(1650)$	$\Lambda(1800)$	$\Sigma(1750)$		
$(70, 1_1^-) \frac{7}{2}^-$		$N(1700)$	-	-		
$(56, 0_2^+) \frac{1}{2}^+$		$N(1675)$	$\Lambda(1830)$	$\Sigma(1775)$		
$(56, 0_2^+) \frac{3}{2}^+$		$N(1440)$	$\Lambda(1600)$	$\Sigma(1660)$	$\Delta(1600)$	$\Sigma(1780)$
$(70, 0_2^+) \frac{1}{2}^+$	$\Lambda(1710)$	$N(1710)$	$\Lambda(1810)$	$\Sigma(1880)$	$\Delta(1750)$	-
$(70, 0_2^+) \frac{3}{2}^+$		-	-	-		
$(56, 2_2^+) \frac{1}{2}^+$		$N(1720)$	$\Lambda(1890)$	$\Sigma(1940)$		
$(56, 2_2^+) \frac{3}{2}^+$		$N(1680)$	$\Lambda(1820)$	$\Sigma(1915)$	$\Delta(1910)$	-
$(56, 2_2^+) \frac{5}{2}^+$					$\Delta(1920)$	$\Sigma(2080)$
$(56, 2_2^+) \frac{7}{2}^+$					$\Delta(1905)$	$\Sigma(2070)$
$(70, 2_2^+) \frac{1}{2}^+$					$\Delta(1950)$	$\Sigma(2030)$
$(70, 2_2^+) \frac{3}{2}^+$	$\Lambda(2070)$	-	-	-	-	-
$(70, 2_2^+) \frac{5}{2}^+$	$\Lambda(2110)$	$N(1860)$	-	-	$\Delta(2000)$	-
$(70, 2_2^+) \frac{7}{2}^+$		$N(1880)$	-	-		
$(70, 2_2^+) \frac{9}{2}^+$		$N(1900)$	-	-		
$(70, 2_2^+) \frac{11}{2}^+$		$N(2000)$	-	-		
$(70, 2_2^+) \frac{13}{2}^+$		$N(1990)$	$\Lambda(2085)$	-		
$(20, 1_2^+) \frac{1}{2}^+$	-	-	-	-		
$(20, 1_2^+) \frac{3}{2}^+$	-	-	-	-		
$(20, 1_2^+) \frac{5}{2}^+$	-	-	-	-		
$(56, 1_3^-) \frac{1}{2}^-$		$N(1895)$	$\Lambda(2000)$	$\Sigma(1900)^a$	$\Delta(1900)$	$\Sigma(2110)^a$
$(56, 1_3^-) \frac{3}{2}^-$		$N(1875)$	$\Lambda(2050)$	$\Sigma(1910)^a$	$\Delta(1940)$	$\Sigma(2100)^a$
$(56, 1_3^-) \frac{5}{2}^-$					$\Delta(1930)$	-
$(70, 3_3^-) \frac{1}{2}^-$	$\Lambda(2080)$	$N(2060)^b$	-	-	-	-
$(70, 3_3^-) \frac{3}{2}^-$	$\Lambda(2100)$	$N(2190)^b$	-	$\Sigma(2100)$	$\Delta(2200)$	-
$(70, 3_3^-) \frac{5}{2}^-$		$N(2120)$	-	-	-	-
$(70, 3_3^-) \frac{7}{2}^-$		$N(2060)^b$	-	-	-	-
$(70, 3_3^-) \frac{9}{2}^-$		$N(2190)^b$	-	-	-	-
$(70, 3_3^-) \frac{11}{2}^-$		$N(2290)$	-	-	-	-

$\Lambda(1830)5/2^-$ and $\Sigma(1775)5/2^-$. The doublet of negative-parity decuplet Σ states is not uniquely identified. Expected is this doublet at about 1750 MeV, and in the $(56, 1_3^-)$ -configuration a second doublet at about 2050 MeV and, finally, a triplet at about the same mass. The analysis found (poor) evidence for two doublets, marked^a in Table 2. The singlet states $\Lambda(1405)1/2^-$ and $\Lambda(1520)3/2^-$ deserve a more detailed discussion.

At higher masses, some choices are a bit arbitrary: Because of its mass, $N(1900)3/2^+$ belongs to the second excitation shell. It may have intrinsic quark spin $1/2$ or $3/2$, both with $L = 2$. Further, there should be a $3/2^+$

⁷ The $N(1700)3/2^-$ is wider than its spin partners and more difficult to identify. This may also be the reason for the absence of the $J^P = 3/2^-$ Λ and Σ states.

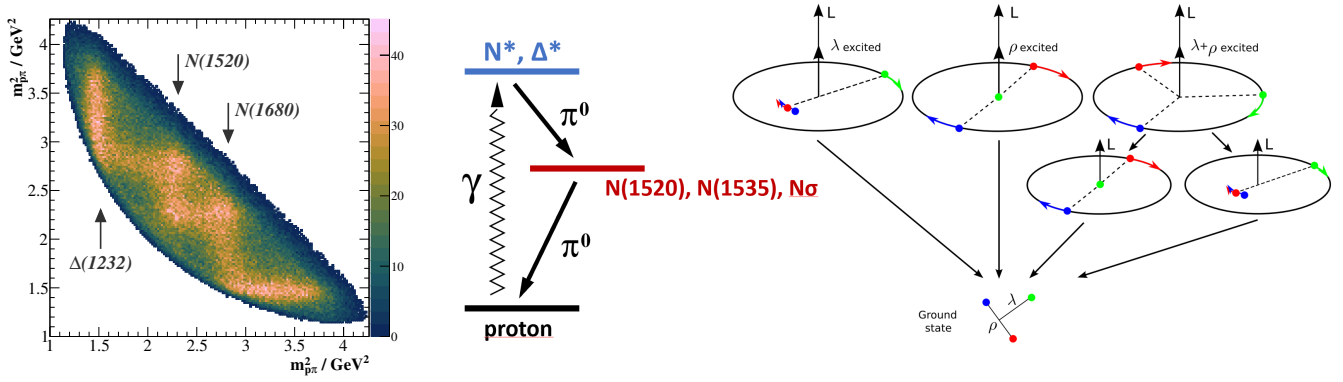


Fig. 5. Left: $\gamma p \rightarrow p\pi^0\pi^0$ -Dalitz plot for a selected E_γ -bin of 1900-2100 MeV (CBELSA/TAPS) [56], Middle: Cascade decays of resonances via an immediate state. Right: Classical orbits of nucleon excitations with $L = 2$ (upper row) and $L = 1$ (middle row). Taken from [37]. The first two pictures in the upper row show excitations of the ρ and λ oscillators, in the third picture both, ρ and λ are excited. When both oscillators are excited, de-excitation leads to an excited intermediate state (middle row).

radially excited state with $L = 0$. These three states can mix. Only one of the states is clearly identified. In any case, quark models predict three resonances with $J^P = 3/2^+$ in this mass range while only one is found. Also missing is a doublet of states with $L = 1$ belonging to the 20plet in $SU(6) \otimes O(3)$.⁸ The production of this doublet is expected to be strongly suppressed for reasons to be discussed below.

Only few hyperons are known that can be assigned to the second excitation shell. The interpretation of some Λ resonances as $SU(3)$ singlet configuration is plausible but not at all compelling.

7.2 Missing resonances

In the spectrum of N^* and Δ^* , the first excitation shell is complete, in the second shell, 21 states are expected (two of them likely not observable in πN -elastic scattering or in single/double meson photoproduction), 16 are seen, three are missing. To a large extent, the *missing-resonance* problem is solved for N^* and Δ^* : there are no frozen diquarks. Admittedly, five of the resonances are not yet “established”, i.e. have not (yet?) a 3^* or 4^* status.

In the third shell, only few resonances are known, but the number of expected resonances is quite large and the analysis challenging: 45 N^* and Δ^* , likely with widths often exceeding 300 MeV, are expected to populate an about 400 MeV wide mass range.

J^P	1. shell	2. shell	3. shell
Masses	1500 - 1750	1700 - 2100	1900 - 2300
N	5: 2 2 1	13: 4 5 3 1	30: 7 9 8 5 1
Δ	2: 1 1 -	8: 2 3 2 1	15: 3 5 4 2 1

⁸ The RPP lists three more N^*/Δ^* -resonances: $N(2040)3/2^+$, $\Delta(2150)1/2^-$, which need confirmation and $N(2100)1/2^+$ which we assign to the 4th shell.

7.3 Three-quark dynamics in cascade decays

The CBELSA/TAPS collaboration studied cascade decays of high mass resonances via an intermediate resonance down to the ground state nucleon. The analyses were based on a large data base of photoproduction data including final states such as $\gamma p \rightarrow p\pi^0\pi^0$ and $p\pi^0\eta$ (see [33, 36] and Refs. therein). The Dalitz plot of Fig. 5, shows very clearly band-like structures due to the occurrence of baryon resonances in the intermediate state. It was observed that the positive parity N^* - and Δ^* -resonances at a mass of about 1900 MeV show a very different decay pattern. The four N^* -resonances $N(1880)1/2^+$, $N(1900)3/2^+$, $N(2000)5/2^+$, $N(1990)7/2^+$ decay with an average branching fraction of $(34 \pm 6)\%$ into $N\pi$ and $\Delta\pi$ and with a branching fraction of $(21 \pm 5)\%$ into the orbitally excited states $N(1520)3/2^-\pi$, $N(1535)1/2^-\pi$, and $N\sigma$. The four Δ^* -states, $\Delta(1910)1/2^+$, $\Delta(1920)3/2^+$, $\Delta(1905)5/2^+$ and $\Delta(1950)7/2^+$ have an average decay branching fraction into $N\pi/\Delta\pi$ of $(44 \pm 7)\%$ while their branching fraction into the excited states mentioned above is almost negligible, only $(5 \pm 2)\%$ [33]. At the first sight, this is very surprising.

The difference can be traced to the different wave functions. The spin and the flavor wave functions of the four Δ^* -states are both symmetric with respect to the exchange of any two quarks, the spatial wave function needs to be symmetric as well. This means that - having a three-quark-picture in mind - that either the ρ - or the λ -oscillator is excited to $\ell = 2$, the other one is not excited. (There is a mixture of the two possibilities $\ell_\rho = 2, \ell_\lambda = 0$ or $\ell_\lambda = 2, \ell_\rho = 0$). If this state decays, the orbital angular momentum is carried away and the decay products are found preferentially in their ground state.

The four N^* -states have a spatial wave function with mixed symmetry. Thus the spatial wave function has one part which is mixed-symmetric and one part which is mixed anti-symmetric. In the latter one, both oscillators are excited simultaneously ($\ell_\rho = \ell_\lambda = 1$). If this state decays, one of the excitations remains in the decay product as illustrated in Fig. 5. A similar argument has been

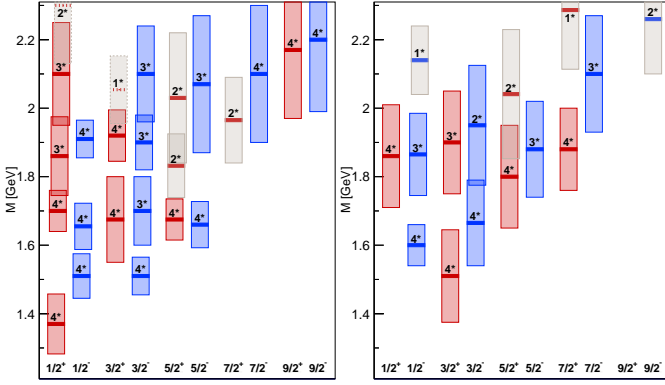


Fig. 6. N^* - (left) and Δ^* -resonances (right) above $\Delta(1232)$ for different spin and parities J^P . For each resonance, the real part of the pole position $Re(M_R)$ is given together with a box of length $\pm Im(M_R)$, using the PDG estimates. $2 \cdot Im(M_R)$ corresponds to the total width of the resonance. RPP star ratings are also indicated. If no pole positions are given in the RPP (above the line), the RPP Breit-Wigner estimates for masses and widths are used instead. This is indicated by dashed resonance-mass lines and dashed lines surrounding the boxes. If no RPP-estimates are given, the values above the line have been averaged and the states are shown as gray boxes. This may indicate one measurement above the line only. $\Delta(1750)1/2^+$ is not included, as there is no RPP-value given above the line.

used by Hey and Kelly [57] to explain why the 20^+ plet in the second excitation shell of Fig. 2 cannot be formed in a πN scattering experiment. For the 20^+ plet the spacial wave function is entirely antisymmetric, both oscillators are excited simultaneously, and there is no other component in the wave function. A single-step excitation is suppressed.

7.4 Parity doublets?

The spontaneous breaking of the chiral symmetry leads to the large mass gap observed between chiral partners: the masses of the $\rho(770)$ meson with spin-parity $J^P = 1^-$ and its chiral partner $a_1(1260)$ with $J^P = 1^+$ differ by about 500 MeV, those of the $J^P = 1/2^+$ nucleon and $N(1535)1/2^-$ by about 600 MeV. In contrast to quark-models expectations and lattice QCD calculations [53] higher-mass baryons are often observed in parity doublets (see Fig. 6), in pairs of resonances having about the same mass, the same total spin J and opposite parities. This observation and similar observations in meson spectrum has led to the suggestion that chiral symmetry might be effectively restored in highly excited hadrons [58, 59]. Then, all high-mass resonances should have a parity partner. This is a testable prediction.

In the mass region of 1900 MeV a quartet of well known positive parity Δ^* states exists, consisting of $\Delta(1910)1/2^+$, $\Delta(1920)3/2^+$, $\Delta(1905)5/2^+$, and $\Delta(1950)7/2^+$. Figure 6 shows the parity partners of the first three states: $\Delta(1900)1/2^-$, $\Delta(1940)3/2^-$, and $\Delta(1930)5/2^-$. However, the four-star $\Delta(1950)7/2^+$ has no close-by $\Delta(???)7/2^-$ -state that

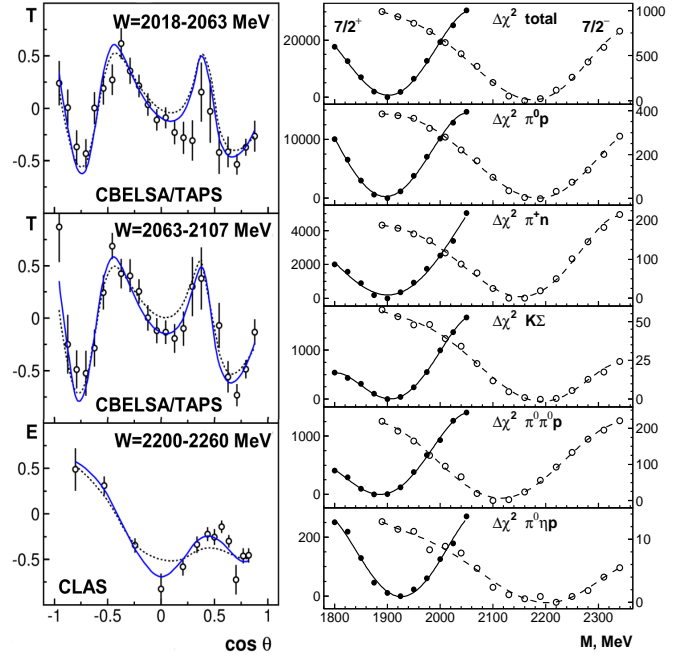


Fig. 7. Left: The new polarization observables T and E shown for selected mass bins (see [35] for refs. to the data). The fit curves represent the best fits with (solid) and without (dashed) inclusion of $\Delta(2200)7/2^-$. Right: The increase in pseudo- χ^2 of the fit to a large body of pion- and photo-produced reactions when the mass of $\Delta(1950)7/2^+$ (solid points) or $\Delta(2200)7/2^-$ (open circles) is scanned. The scale on the left (right) abscissa refers to the $7/2^+$ ($7/2^-$) partial wave. The curves are to guide the eye. Adapted/taken from [35].

could serve as parity partner. Where is the closest Δ^* with $J^P = 7/2^-$? Figure 7 shows a resonance scan over the mass region of interest [35]. There is clear evidence for $\Delta(2200)7/2^-$ (which was upgraded from 1^* to 3^* based on this result). But its mass difference to $\Delta(1950)7/2^+$ is too large. These two states are no parity partners!

Within the quark model and the $SU(6) \otimes O(3)$ -systematics, the four positive-parity Δ^* 's have $L = 2, S = 3/2$ that couple to $J^P = 1/2^+, \dots, 7/2^+$. The natural assignment for the three negative-parity Δ^* 's is that they form a triplet with $L = 1$ and $S = 3/2$. Then, they must have one unit of radial excitation. The four positive-parity Δ -states belong to the $2\hbar\omega$ shell and the negative-parity states to the $3\hbar\omega$ shell. With masses considered to be proportional to $L + N_{\text{radial}}$, these seven states are expected to have about the same mass. $\Delta(2200)7/2^-$ has $L = 3, S = 1/2$ and its expected mass is higher. We note that $\Delta(2400)9/2^-$ has $L = 3, S = 3/2$, and we assume $N_{\text{radial}} = 1$ for this state (as well as for $\Delta(2750)13/2^-$, see Fig. 4).

8 Dynamically generated resonances

8.1 N^* 's and Δ^* 's

Apart from $\Lambda(1405)1/2^-$ that will be discussed below, the first dynamically generated resonance was the nega-

tive-parity $N(1535)1/2^-$ [28]. At the 1995 International Conference on the Structure of Baryons, Santa Fe, New Mexico, there was a heated discussion between Weise, defending his new approach, and Isgur who argued that $N(1535)1/2^-$ is well understood within the quark model and no new approach is needed. For some time, there was even the idea that there could be two overlapping states but this is excluded by data. Later, in [60,61] $N(1535)1/2^-$ and $N(1650)1/2^-$, were both shown to be generated dynamically but not $\Delta(1620)1/2^-$ ⁹. An important question remains: Are (qqq)-resonance poles and dynamically generated poles different descriptions of the same object or do they present different (orthogonal) states?

8.2 The $\Lambda(1405)1/2^-$

The $\Lambda(1405)1/2^-$ mass is very close to the $N\bar{K}$ threshold. Kaiser, Waas and Weise [62] proved that the resonance can be generated dynamically from $N\bar{K} - \Sigma\pi$ coupled-channel dynamics. Oller and Meissner [63] studied the S -wave $N\bar{K}$ interactions in a relativistic chiral unitary approach based on a chiral Lagrangian obtained from the interaction of the octet of pseudoscalar mesons and the ground state baryon octet and found two isoscalar resonances in the $\Lambda(1405)1/2^-$ mass region and one isovector state. In a subsequent paper [64], Jido *et al.* studied the effects of SU(3) breaking on the results in detail. These two papers had an immense impact on the further development. It is the only result in light-baryon spectroscopy that is in clear contradiction to the quark model. It introduces a new state $\Lambda(1380)1/2^-$, that has no role in a quark model, it enforces an interpretation of $\Lambda(1405)1/2^-$ as mainly SU(3) octet resonance, and it interprets $\Lambda(1670)1/2^-$ as high-mass partner of $\Lambda(1405)1/2^-$. The $\Lambda(1405)1/2^-$ and $\Lambda(1670)1/2^-$ would then be the strange partners of the $N(1535)1/2^-$ and the $N(1650)1/2^-$. In quark models, $\Lambda(1405)1/2^-$ is a mainly SU(3) singlet resonance and the octet states $\Lambda(1670)1/2^-$ and $\Lambda(1800)1/2^-$ are the strange partners of $N(1535)1/2^-$ and $N(1650)1/2^-$ (see Table 2). In the quark-model interpretation, the hyperon states $\Lambda(1405)1/2^-$ and $\Lambda(1670)1/2^-$ have close-by $J^P = 3/2^-$ partners (the $J^P = 3/2^-$ -partner of $\Lambda(1800)1/2^-$ is missing but there is $\Lambda(1830)5/2^-$). The masses of the mainly octet states are about 130 MeV above their non-strange partners.

This conflict initiated an attempt to fit (nearly) all existing data relevant for $\Lambda(1405)1/2^-$ in the BnGa approach [65]. The data could be fit with one single resonance in the $\Lambda(1405)1/2^-$ region but were also compatible, with a slightly worsened χ^2 , with a description using two resonances with properties as obtained in the chiral unitary approach.

⁹ It should be mentioned that not only the SU(6)⊗O(3)-systematics in the spectrum seems to indicate a 3-quark-nature of $N(1535)1/2^-$ and $N(1650)1/2^-$ but also the electroproduction results discussed in the following section ?? indicate that $N(1535)1/2^-$ is a 3-quark state with little meson-baryon contribution only (Q^2 dependence of the transition form factor $A_{1/2}$).

9 Outlook

There is not yet a unified picture of baryons. Regge-like trajectories ($M^2 \propto L + N_{\text{radial}}$) are best described by AdS/QCD. Unitary effective field theories describe consistently meson-baryon interactions and some resonances are generated dynamically from their interaction. The quark model is useful to understand cascade decays of highly excited states and is indispensable to discuss the full spectrum including missing resonances. The symmetry of quark pairs, symmetric or anti-symmetric with respect to their exchange, has a significant impact on baryon masses. They could be due to effective gluon exchange. More likely seems an interpretation by quark and gluon condensates, e.g. by instanton-induced interactions. Based on the new high quality (polarized) photoproduction data, new baryon resonances were discovered and our knowledge of properties of existing resonances has increased considerably. Yet, our understanding is still unsatisfactory mirroring the complexity of QCD in the non-perturbative regime. New results from lattice QCD are eagerly awaited and new experiments are needed to understand the spectrum and the properties of baryon resonances in further detail. Those include further precise photoproduction experiments measuring polarisation observables not only off the proton but also off the neutron as well as multi-meson final states. Strange baryon resonances need to be addressed. Other production processes such as electroproduction, $\bar{p}p$ -annihilation, experiments with π^- or K^- -beams and baryon resonances produced in J/ψ or ψ' -decays will also contribute to improve our understanding of the bound states of the strong interaction.

References

1. N. Isgur, “Why N^* ’s are important,” 7 2000.
2. N. Isgur and G. Karl, “Hyperfine Interactions in Negative Parity Baryons,” *Phys. Lett. B*, vol. 72, p. 109, 1977.
3. S. Capstick and N. Isgur, “Baryons in a relativized quark model with chromodynamics,” *Phys. Rev. D*, vol. 34, no. 9, pp. 2809–2835, 1986.
4. U.-G. Meißner, “Towards a theory of baryon resonances,” *EPJ Web Conf.*, vol. 241, p. 02003, 2020.
5. G. Hohler, F. Kaiser, R. Koch, and E. Pietarinen, *Handbook of pion nucleon scattering*, vol. 12N1. 1979.
6. R. E. Cutkosky, C. P. Forsyth, R. E. Hendrick, and R. L. Kelly, “Pion - Nucleon Partial Wave Amplitudes,” *Phys. Rev. D*, vol. 20, p. 2839, 1979.
7. R. A. Arndt, W. J. Briscoe, I. I. Strakovsky, and R. L. Workman, “Extended partial-wave analysis of πN scattering data,” *Phys. Rev. C*, vol. 74, p. 045205, 2006.
8. L. Tiator, M. Gorchtein, V. L. Kashevarov, K. Nikonov, M. Ostrick, M. Hadžimehmedović, R. Omerović, H. Osmanović, J. Stahov, and A. Švarc, “Eta and Etaprime Photoproduction on the Nucleon with the Isobar Model EtaMAID2018,” *Eur. Phys. J. A*, vol. 54, no. 12, p. 210, 2018.
9. V. L. Kashevarov *et al.*, “Study of η and η' Photoproduction at MAMI,” *Phys. Rev. Lett.*, vol. 118, no. 21, p. 212001, 2017.

10. F. Afzal *et al.*, “Observation of the $p\eta'$ Cusp in the New Precise Beam Asymmetry Σ Data for $\gamma p \rightarrow p\eta$,” *Phys. Rev. Lett.*, vol. 125, no. 15, p. 152002, 2020.
11. J. Müller *et al.*, “New data on $\bar{\gamma}p \rightarrow \eta p$ with polarized photons and protons and their implications for $N^* \rightarrow N\eta$ decays,” *Phys. Lett. B*, vol. 803, p. 135323, 2020.
12. I. Senderovich *et al.*, “First measurement of the helicity asymmetry E in η photoproduction on the proton,” *Phys. Lett. B*, vol. 755, pp. 64–69, 2016.
13. S. Capstick and W. Roberts, “Quasi two-body decays of nonstrange baryons,” *Phys. Rev. D*, vol. 49, pp. 4570–4586, 1994.
14. A. V. Anisovich, V. Burkert, P. M. Collins, M. Dugger, E. Klempt, V. A. Nikonov, B. G. Ritchie, A. V. Sarantsev, and U. Thoma, “ $N^* \rightarrow N\eta'$ decays from photoproduction of η' -mesons off protons,” *Phys. Lett. B*, vol. 772, pp. 247–252, 2017.
15. A. V. Anisovich, V. Burkert, M. Dugger, E. Klempt, V. A. Nikonov, B. G. Ritchie, A. V. Sarantsev, and U. Thoma, “Proton- η' interactions at threshold,” *Phys. Lett. B*, vol. 785, pp. 626–630, 2018.
16. A. V. Anisovich, R. Beck, E. Klempt, V. A. Nikonov, A. V. Sarantsev, and U. Thoma, “Properties of baryon resonances from a multichannel partial wave analysis,” *Eur. Phys. J. A*, vol. 48, p. 15, 2012.
17. M. E. McCracken *et al.*, “Differential cross section and recoil polarization measurements for the $\gamma p \rightarrow K^+ \Lambda$ reaction using CLAS at Jefferson Lab,” *Phys. Rev. C*, vol. 81, p. 025201, 2010.
18. B. Dey *et al.*, “Differential cross sections and recoil polarizations for the reaction $\gamma p \rightarrow K^+ \Sigma^0$,” *Phys. Rev. C*, vol. 82, p. 025202, 2010.
19. C. A. Paterson *et al.*, “Photoproduction of Λ and Σ^0 hyperons using linearly polarized photons,” *Phys. Rev. C*, vol. 93, no. 6, p. 065201, 2016.
20. A. Thiel, F. Afzal, and Y. Wunderlich, “Light Baryon Spectroscopy,” *Prog. Part. Nucl. Phys.*, vol. 125, p. 103949, 2022.
21. H. Osmanović, M. Hadžimehmedović, R. Omerović, J. Stahov, M. Gorchtein, V. Kashevarov, K. Nikonov, M. Ostrick, L. Tiator, and A. Švarc, “Single-energy partial wave analysis for π^0 photoproduction on the proton with fixed- t analyticity imposed,” *Phys. Rev. C*, vol. 100, no. 5, p. 055203, 2019.
22. H. Osmanović, M. Hadžimehmedović, R. Omerović, J. Stahov, V. Kashevarov, M. Ostrick, L. Tiator, and A. Švarc, “Single-energy partial-wave analysis for pion photoproduction with fixed- t analyticity,” *Phys. Rev. C*, vol. 104, no. 3, p. 034605, 2021.
23. A. V. Anisovich *et al.*, “Strong evidence for nucleon resonances near 1900 MeV,” *Phys. Rev. Lett.*, vol. 119, no. 6, p. 062004, 2017.
24. J. Hartmann *et al.*, “The $N(1520)3/2^-$ helicity amplitudes from an energy-independent multipole analysis based on new polarization data on photoproduction of neutral pions,” *Phys. Rev. Lett.*, vol. 113, p. 062001, 2014.
25. A. Švarc, Y. Wunderlich, and L. Tiator, “Application of the single-channel, single-energy amplitude and partial-wave analysis method to $K^+ \Lambda$ photoproduction,” *Phys. Rev. C*, vol. 105, no. 2, p. 024614, 2022.
26. D. Rönchen, M. Döring, U.-G. Meißner, and C.-W. Shen, “Light baryon resonances from a coupled-channel study including $K\Sigma$ photoproduction,” 7 2022.
27. N. Isgur and G. Karl, “P Wave Baryons in the Quark Model,” *Phys. Rev. D*, vol. 18, p. 4187, 1978.
28. N. Kaiser, P. B. Siegel, and W. Weise, “Chiral dynamics and the S11 (1535) nucleon resonance,” *Phys. Lett. B*, vol. 362, pp. 23–28, 1995.
29. A. V. Anisovich *et al.*, “The impact of new polarization data from Bonn, Mainz and Jefferson Laboratory on $\gamma p \rightarrow \pi N$ multipoles,” *Eur. Phys. J. A*, vol. 52, no. 9, p. 284, 2016.
30. R. L. Workman, M. W. Paris, W. J. Briscoe, and I. I. Strakovsky, “Unified Chew-Mandelstam SAID analysis of pion photoproduction data,” *Phys. Rev. C*, vol. 86, p. 015202, 2012.
31. B. C. Hunt and D. M. Manley, “Updated determination of N^* resonance parameters using a unitary, multichannel formalism,” *Phys. Rev. C*, vol. 99, no. 5, p. 055205, 2019.
32. B. Julia-Diaz, T. S. H. Lee, A. Matsuyama, and T. Sato, “Dynamical coupled-channel model of πN scattering in the $W \leq 2$ -GeV nucleon resonance region,” *Phys. Rev. C*, vol. 76, p. 065201, 2007.
33. T. Seifen *et al.*, “Polarization observables in double neutral pion photoproduction,” 7 2022.
34. H. Kamano, T. S. H. Lee, S. X. Nakamura, and T. Sato, “The ANL-Osaka Partial-Wave Amplitudes of πN and γN Reactions,” 9 2019.
35. A. V. Anisovich, V. Burkert, J. Hartmann, E. Klempt, V. A. Nikonov, E. Pasyuk, A. V. Sarantsev, S. Strauch, and U. Thoma *Phys. Lett. B*, vol. 766, pp. 357–361, 2017.
36. E. Gutz *et al.*, “High statistics study of the reaction $\gamma p \rightarrow p\pi^0\eta$,” *Eur. Phys. J. A*, vol. 50, p. 74, 2014.
37. A. Thiel *et al.*, “Three-body nature of N^* and Δ^* resonances from sequential decay chains,” *Phys. Rev. Lett.*, vol. 114, no. 9, p. 091803, 2015.
38. U. Loring, B. C. Metsch, and H. R. Petry, “The Light baryon spectrum in a relativistic quark model with instanton induced quark forces: The Nonstrange baryon spectrum and ground states,” *Eur. Phys. J. A*, vol. 10, pp. 395–446, 2001.
39. E. Klempt, “A Mass formula for baryon resonances,” *Phys. Rev. C*, vol. 66, p. 058201, 2002.
40. H. Forkel and E. Klempt, “Diquark correlations in baryon spectroscopy and holographic QCD,” *Phys. Lett. B*, vol. 679, pp. 77–80, 2009.
41. E. Klempt, “Nucleon Excitations,” *Chin. Phys. C*, vol. 34, no. 9, pp. 1241–1246, 2010.
42. E. Klempt, “Delta resonances, Quark models, chiral symmetry and AdS/QCD,” *Eur. Phys. J. A*, vol. 38, pp. 187–194, 2008.
43. S. Prakhov *et al.*, “Measurement of $\pi^0 \Lambda$, $\bar{K}^0 n$, and $\pi^0 \Sigma^0$ production in $K^- p$ interactions for p_{K^-} between 514 and 750-MeV/c,” *Phys. Rev. C*, vol. 80, p. 025204, 2009.
44. K. Moriya *et al.*, “Measurement of the $\Sigma\pi$ photoproduction line shapes near the $\Lambda(1405)$,” *Phys. Rev. C*, vol. 87, no. 3, p. 035206, 2013.
45. H. Zhang, J. Tulpan, M. Shrestha, and D. M. Manley, “Partial-wave analysis of $\bar{K}N$ scattering reactions,” *Phys. Rev. C*, vol. 88, no. 3, p. 035204, 2013.
46. H. Zhang, J. Tulpan, M. Shrestha, and D. M. Manley, “Multichannel parametrization of $\bar{K}N$ scattering amplitudes and extraction of resonance parameters,” *Phys. Rev. C*, vol. 88, no. 3, p. 035205, 2013.
47. C. Fernandez-Ramirez, I. V. Danilkin, D. M. Manley, V. Mathieu, and A. P. Szczepaniak, “Coupled-channel

- model for $\bar{K}N$ scattering in the resonant region,” *Phys. Rev. D*, vol. 93, no. 3, p. 034029, 2016.
48. H. Kamano, S. X. Nakamura, T. S. H. Lee, and T. Sato, “Dynamical coupled-channels model of K^-p reactions: Determination of partial-wave amplitudes,” *Phys. Rev. C*, vol. 90, no. 6, p. 065204, 2014.
 49. H. Kamano, S. X. Nakamura, T. S. H. Lee, and T. Sato, “Dynamical coupled-channels model of K^-p reactions. II. Extraction of Λ^* and Σ^* hyperon resonances,” *Phys. Rev. C*, vol. 92, no. 2, p. 025205, 2015. [Erratum: *Phys. Rev. C* 95, 049903 (2017)].
 50. M. Matveev, A. V. Sarantsev, V. A. Nikonov, A. V. Anisovich, U. Thoma, and E. Klempt, “Hyperon I: Partial-wave amplitudes for K^-p scattering,” *Eur. Phys. J. A*, vol. 55, no. 10, p. 179, 2019.
 51. A. V. Sarantsev, M. Matveev, V. A. Nikonov, A. V. Anisovich, U. Thoma, and E. Klempt, “Hyperon II: Properties of excited hyperons,” *Eur. Phys. J. A*, vol. 55, no. 10, p. 180, 2019.
 52. E. Klempt, V. Burkert, U. Thoma, L. Tiator, and R. Workman, “ Λ and Σ Excitations and the Quark Model,” *Eur. Phys. J. A*, vol. 56, no. 10, p. 261, 2020.
 53. R. G. Edwards, J. J. Dudek, D. G. Richards, and S. J. Wallace, “Excited state baryon spectroscopy from lattice QCD,” *Phys. Rev. D*, vol. 84, p. 074508, 2011.
 54. G. Eichmann and C. S. Fischer, “Baryon Structure and Reactions,” *Few Body Syst.*, vol. 60, no. 1, p. 2, 2019.
 55. S. J. Brodsky, G. F. de Teramond, H. G. Dosch, and J. Erlich, “Light-Front Holographic QCD and Emerging Confinement,” *Phys. Rept.*, vol. 584, pp. 1–105, 2015.
 56. P. Mahlberg *PhD-thesis Bonn, in preparation*, vol. 114, no. 9, p. 091803, 2023.
 57. A. J. G. Hey and R. L. Kelly, “Baryon spectroscopy,” *Phys. Rept.*, vol. 96, p. 71, 1983.
 58. L. Y. Glozman, “Parity doublets and chiral symmetry restoration in baryon spectrum,” *Phys. Lett. B*, vol. 475, pp. 329–334, 2000.
 59. L. Y. Glozman, “Chiral multiplets of excited mesons,” *Phys. Lett. B*, vol. 587, pp. 69–77, 2004.
 60. P. C. Bruns, M. Mai, and U. G. Meissner, “Chiral dynamics of the $S_{11}(1535)$ and $S_{11}(1650)$ resonances revisited,” *Phys. Lett. B*, vol. 697, pp. 254–259, 2011.
 61. M. Mai, P. C. Bruns, and U.-G. Meissner, “Pion photoproduction off the proton in a gauge-invariant chiral unitary framework,” *Phys. Rev. D*, vol. 86, p. 094033, 2012.
 62. N. Kaiser, T. Waas, and W. Weise, “SU(3) chiral dynamics with coupled channels: Eta and kaon photoproduction,” *Nucl. Phys. A*, vol. 612, pp. 297–320, 1997.
 63. J. A. Oller and U. G. Meissner, “Chiral dynamics in the presence of bound states: Kaon nucleon interactions revisited,” *Phys. Lett. B*, vol. 500, pp. 263–272, 2001.
 64. D. Jido, J. A. Oller, E. Oset, A. Ramos, and U. G. Meissner, “Chiral dynamics of the two $\Lambda(1405)$ states,” *Nucl. Phys. A*, vol. 725, pp. 181–200, 2003.
 65. A. V. Anisovich, A. V. Sarantsev, V. A. Nikonov, V. Burkert, R. A. Schumacher, U. Thoma, and E. Klempt, “Hyperon III: $K^-p - \pi\Sigma$ coupled-channel dynamics in the $\Lambda(1405)$ mass region,” *Eur. Phys. J. A*, vol. 56, no. 5, p. 139, 2020.